Substrate Binding Stabilizes *S*-Adenosylhomocysteine Hydrolase in a Closed Conformation†

Dan Yin,‡ Xiaoda Yang,‡ Yongbo Hu,‡ Krysztof Kuczera,§ Richard L. Schowen,‡,§ Ronald T. Borchardt,‡ and Thomas C. Squier*,§

Department of Pharmaceutical Chemistry and Biochemistry and Biophysics Section, Department of Molecular Biosciences, University of Kansas, Lawrence, Kansas 66045

Received March 15, 2000; Revised Manuscript Received May 24, 2000

ABSTRACT: Comparison of crystal structures of *S*-adenosylhomocysteine (AdoHcy) hydrolase in the substrate-free, NAD^+ form [Hu, Y., Komoto, J., Huang, Y., Gomi, T., Ogawa, H., Takata, Y., Fujioka, M., and Takusagawa, F. (1999) *Biochemistry* 38, 8323−8333] and a substrate-bound, NADH form [Turner, M. A., Yuan, C.-S., Borchardt, R. T., Hershfield, M. S., Smith, G. D., and Howell, P. L. (1998) *Nat. Struct. Biol.* 5, 369−376] indicates large differences in the spatial arrangement of the catalytic and NAD^+ binding domains. The substrate-free, NAD^+ form exists in an "open" form with respect to catalytic and NAD^+ binding domains, whereas the substrate-bound, NADH form exists in a closed form with respect to those domains. To address whether domain closure is induced by substrate binding or its subsequent oxidation, we have measured the rotational dynamics of spectroscopic probes covalently bound to Cys^{113} and Cys^{421} within the catalytic and carboxyl-terminal domains. An independent domain motion is associated with the catalytic domain prior to substrate binding, suggesting the presence of a flexible hinge element between the catalytic and NAD^+ binding domains. Following binding of substrates (i.e., adenosine or neplanocin A) or a nonsubstrate (i.e., 3′-deoxyadenosine), the independent domain motion associated with the catalytic domain is essentially abolished. Likewise, there is a substantial decrease in the average hydrodynamic volume of the protein that is consistent with a reduction in the overall dimensions of the homotetrameric enzyme following substrate binding and oxidation observed in earlier crystallographic studies. Thus, the catalytic and NAD^+ binding domains are stabilized to form a closed active site through interactions with the substrate prior to substrate oxidation.

Critical to a host of intracellular methylation reactions is the hydrolysis of *S*-adenosylhomocysteine (AdoHcy),[1] which is formed following transfer of an activated methyl group from *S*-adenosylmethionine (AdoMet) (*1*). In eukaryotes, the only known pathway for the catabolism of AdoHcy is the reversible hydrolysis to adenosine (Ado) and homocysteine (Hcy), which is catalyzed by AdoHcy hydrolase (EC 3.3.1.1) (*2*). Since methyl-transfer reactions are required for the formation of the 5′-capped structures common to many eukaryotic viruses (*3*, *4*), AdoHcy hydrolase is an important target with respect to the development of broad-spectrum antiviral agents (*5*). In addition, elevated plasma homocysteine levels have been implicated as a risk factor for cardiovascular disease (*6*). As a result of these considerations, there is interest in understanding the detailed mechanism by which AdoHcy hydrolase carries out catalysis. In this respect, important details regarding the catalytic mechanism are now available because of the recent elucidation of two crystal structures of AdoHcy hydrolase isoforms from human and rat, which possess 97% sequence identity (*7*, *8*). In the case of the rat enzyme, the structure was solved in the substrate-free form. In the case of the human enzyme structure, the enzyme was associated with the Ado analogue 2′,3′-dihydroxycyclopent-4′-enyladenine (DHCeA), which serves as a substrate for the oxidative activity of the enzyme generating the 3′-keto analogue and arrests the enzyme in the NADH form.

AdoHcy hydrolase is a homotetramer; each subunit contains three domain elements and a tightly bound NAD^+ cofactor whose redox properties promote the hydrolysis of AdoHcy (Figure 1). The three domain elements consist of a large catalytic domain (domain I), the NAD^+ binding domain (domain II), and a small carboxyl-terminal domain (domain C). The large catalytic domain contains a binding site for AdoHcy and in the human isoform consists of amino acids 1−182 and 353−403 (*7*, *8*). This domain is structurally homologous to that of the catalytic domains of a number of

† Supported in part by grants from the National Institutes of Health (GM29332) and a postdoctoral fellowship to D.Y. from the American Heart Association Heartland Affiliate (9920522Z). The tandem mass spectrometer and electrospray source were respectively obtained through grants from the National Institutes of Health (S10 RR0 6294) and the National Science Foundation (CHE-9413975).

* To whom correspondence should be addressed. Telephone: (785) 864-4008. Fax (785) 864-5321. E-mail: tsquier@ukans.edu.

‡ Department of Pharmaceutical Chemistry.

§ Biochemistry and Biophysics Section.

[1] Abbreviations: 3′-deoxyAdo, 3′-deoxyadenosine; Ade, adenine; Ado, adenosine; AdoHcy, *S*-adenosylhomocysteine; AdoMet, *S*-adenosylmethionine; buffer A, 50 mM potassium phosphate (pH 7.2), 1.0 mM EDTA; DHCeA, 2′,3′-dihydroxycyclopent-4′-enyladenine; DTNB, 5,5′-dithiobis-2-nitrobenzoic acid; DTT, dithiothreitol; E_{NAD+}, NAD^+ bound AdoHcy hydrolase; E_{NADH}, NADH bound AdoHcy hydrolase; ESI-MS, electron spray ionization mass spectrometry; Hcy, homocysteine; HPLC, high-performance liquid chromatography; IAEDANS, 5-((((2-iodoacetyl)amino)-ethyl)amino)naphthalene-1-sulfonic acid; PMal, *N*-(1-pyrenyl) maleimide; NepA, neplanocin A.

10.1021/bi000595a CCC: $19.00
Published on Web 07/14/2000

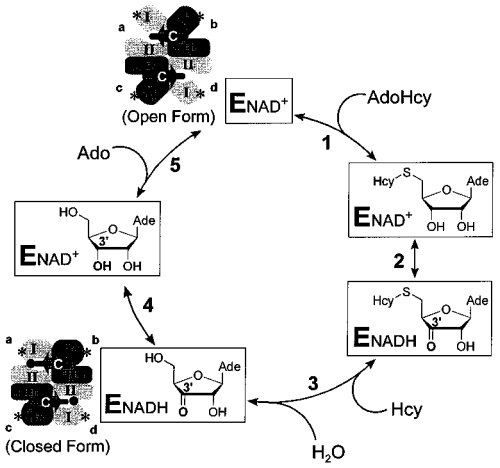

FIGURE 1: Schematic depiction of catalytic mechanism of AdoHcy hydrolase. Cartoons represent the crystal structures of the homotetrameric enzyme in different forms. Each subunit (a, b, c, and d) contains three domains, termed the catalytic domain (I), the NAD^+ binding domain (II), and the carboxyl-terminal domain (C). Two of the four cofactors are shown (solid bars). Enzyme-bound substrate is represented by black dot. The approximate location of Cys^{113} in the catalytic domain is indicated by an asterisk (∗). Discrete steps in the mechanism have been elucidated by Palmer and Abeles (*43*), and written in the physiologically relevant direction of hydrolysis include binding of AdoHcy (step 1), oxidation of the 3′-hydroxyl group of AdoHcy (step 2), and β-elimination of Hcy followed by Michael addition of water on the 5′-position of the tightly bound intermediate (step 3), yielding 3′-ketoAdo. The 3′-ketoAdo is reduced by enzyme-bound NADH to Ado (step 4), which is then released from the NAD^+ form of the enzyme (step 5).

AdoMet-dependent methyltransferases and inosine-uridine *N*-ribohydrolase, and it has been suggested that the substrate can bind to the catalytic site without major changes in the AdoHcy hydrolase structure (*8*). The NAD^+ binding domain consists of amino acids 183−352 and in addition to providing the coenzyme binding crevice, functions as the structural core of the tetrameric complex mediating a multitude of intersubunit interactions. The carboxyl-terminal domain consists of amino acids 404−432 and forms part of the binding pocket for the NAD^+ cofactor of the adjacent subunit, which may be important in stabilizing the quaternary structure of the enzyme (*7*−*9*).

A comparison between the two crystal structures indicates that a hinged domain movement results in large spatial rearrangements with respect to the catalytic domain and NAD^+ binding domain (*7*, *8*). For example, the spatial separation between residues within the catalytic and NAD^+ binding domains in the structure solved by Howell and colleagues following oxidation of DHCeA decreases by as much as 10 Å relative to the substrate-free form of the enzyme. However, from this comparison, it is not clear whether ligand binding or the 3′-oxidation of the substrate results in the observed structural changes in AdoHcy hydrolase (see Figure 1). In the present work, we have used frequency-domain measurements of fluorescence anisotropy to investigate hydrodynamic conformational changes within AdoHcy hydrolase that are associated with binding of nonsubstrate [i.e., 3′-deoxyadenosine (3′-deoxyAdo)] or oxidation at the 3′-position of the ribose of substrates [i.e., Ado and neplanocin A (NepA)].

EXPERIMENTAL PROCEDURES

Materials. 3′-deoxyAdo, 5,5′-dithiobis-2-nitrobenzoic acid (DTNB), dithiothreitol (DTT), NAD^+, sequencing grade α-chymotrypsin (EC 3.4.21.1), and endoproteinase Glu-C (EC 3.4.21.19) were obtained from Sigma (St. Louis, MO). *N*-(1-pyrenyl) maleimide (PMal) and 5-((((2-iodoacetyl)-amino)-ethyl)amino)naphthalene-1-sulfonic acid (IAEDANS) were obtained from Molecular Probes (Eugene, OR). NepA was provided by Dr. Morris Robins (Brigham Young University, Provo, UT). Purification and reconstitution of recombinant human placental AdoHcy hydrolase to the NAD^+ form were previously described by Yuan and coworkers (*10*).

Enzymatic Assays. The assays of AdoHcy hydrolase activity were performed as described previously (*11*). In the synthetic direction, the rate of AdoHcy formation from Ado and Hcy in buffer A [50 mM potassium phosphate (pH 7.2), 1.0 mM EDTA] at 37 °C was measured using a C18 reversed-phase HPLC column (Vydac, Hesperia, CA). In the hydrolytic direction, the rate of Hcy production from AdoHcy was measured spectroscopically by reaction with DTNB in buffer A at 37 °C. The protein concentration was measured using the Bradford assay with bovine serum albumin as a standard (*12*).

Chemical Derivatization of AdoHcy Hydrolase. Selected cysteines on AdoHcy hydrolase (0.3 mg mL^{-1}) were covalently modified following incubation with either 100 μM IAEDANS or 12 μM PMal in the presence of 1 mM Ado in buffer A at 25 °C, essentially as previously described by Yuan and coworkers (*11*). The reaction was quenched after 2 h by the addition of 0.1 mM DTT, prior to separation of the labeled AdoHcy hydrolase from unreacted IAEDANS or PMal using a Sephadex G-25 column (45 × 2.5 cm). To remove enzyme-bound Ado, the eluted protein was dialyzed against buffer A at 4 °C. Incorporation of AEDANS or PMal was determined using the molar extinction coefficient ϵ_{336}(AEDANS) = 5700 M^{-1} cm^{-1} or ϵ_{338} (PMal) = 40 000 M^{-1} cm^{-1} (*13*).

Identification of PMal-Labeled Proteolytic Fragments. Following covalent modification with PMal, sites of chemical modification were identified using electrospray ionization mass spectrometry (ESI-MS) following proteolytic digestion and isolation of the labeled peptides by reversed-phase HPLC, essentially as previously described (*14*, *15*). Briefly, PMal-labeled AdoHcy hydrolase (0.5 mg mL^{-1}) was first digested using chymotrypsin (10 μg mL^{-1}) in 50 mM NH_4HCO_3 (pH 8.0) for 24 h at 37 °C prior to peptide separation using a C18 reversed-phase HPLC column (Vydac 218TP54, 250 × 46 mm) consisting of solvent A (0.1% trifluoroacetic acid) and solvent B (80% acetonitrile, 20% 2-propanol, 0.1% trifluoroacetic acid). Initial conditions were 2% solvent B for 10 min followed by a linear gradient to 62% solvent B over 120 min at a flow rate of 0.5 mL min^{-1}. Following lyophilization of PMal-labeled chymotryptic fragments collected and pooled from the primary separation, a secondary digestion involved the addition of endoproteinase Glu-C in 50 mM potassium phosphate (pH 7.8) for 24 h at 37 °C. Separation of the resulting peptides involved reversed-phase HPLC (see above). Isolated peptides were collected and lyophilized, and the associated masses were measured using ESI-MS, as previously described (*14*). Identification of the

labeled peptides involved the use of the software GPMAW (Lighthouse Data, Aalokken 14, DK-5250, Odense SV, Denmark) for the mass matching in conjunction with the published sequence of human placental AdoHcy hydrolase (*16*).

Fluorescence Measurements. Excitation involved the 351 nm line of an argon ion laser (Coherent Corp., Santa Clara, CA), and emitted fluorescence of either AEDANS or PMal-AdoHcy hydrolase were, respectively, detected after either a Schott GG-420 long-pass filter or a Corion 380 nm interference filter. Lifetime and anisotropy measurements were made using an ISS-K2 fluorometer (ISS Corp., Champaign, IL). Fluorescence intensity or anisotropy decays were fit to a sum of exponentials using the method of nonlinear least-squares (*17*). Alternatively, appropriate expressions have been derived that permit determination of the initial anisotropy (r_o), rotational correlation times (ϕ_i), and the amplitudes of the total anisotropy loss associated with each rotational correlation time ($r_o g_i$). The derivation and application of these expression have been described in detail elsewhere (*18*−*21*). Data were fit using the Globals software package (University of Illinois, Urbana-Champaign). Unless otherwise indicated, data were analyzed using frequency-independent errors in the phase and modulation that were assumed to be 0.2° and 0.005, respectively.

RESULTS

Covalent Modification of AdoHcy Hydrolase with PMal. Each subunit of AdoHcy hydrolase contains 10 cysteine residues. Previous studies have shown that three cysteine residues (i.e., Cys^{113}, Cys^{195}, and Cys^{421}) can be chemically modified using the sulfhydryl-specific reagents DTNB or iodoacetamide (*11*). Cys^{113} and Cys^{195} are protected from modification by DTNB or iodoacetamide in the presence of Ado. Cys^{195} is essential to the catalytic activity, whereas covalent modification of Cys^{113} or Cys^{421} does not affect enzyme function. These results can be rationalized in light of the crystal structure, since Cys^{195} is in the catalytic pocket near the substrate (*7*). In contrast, neither of the other two reactive cysteines is involved in either substrate binding or catalysis. In the structure, Cys^{113} is within a hydrophobic cleft near the surface of the catalytic domain, while Cys^{421} is on the surface of the carboxyl-terminal domain (Figure 1). Therefore, in the presence of Ado it is possible to chemically modify nonessential cysteines on AdoHcy hydrolase using fluorescent probes that permit measurements of the hydrodynamic properties of the enzyme stabilized in different catalytic states. We have, therefore, covalently modified AdoHcy hydrolase with the hydrophobic fluorescent probe PMal in the presence of 1 mM Ado. A total of 1.5 ± 0.2 mol of PMal are incorporated per mole of subunit, indicating that multiple cysteines have been covalently modified. Since there is full retention of both the hydrolytic and synthetic activities following covalent modification with PMal (data not shown), it is likely that both of the chemically reactive nonessential cysteines (i.e., Cys^{113} and Cys^{421}) are modified. However, to facilitate the interpretation of the fluorescence anisotropy data (see below), we have identified the sites of modification by proteolytic digestion of the PMal-labeled enzyme, separation of labeled peptides by reversed-phase HPLC (Figure 2A), and characterization of the peptides by ESI-MS. Three major fluorescent signals are apparent in the chromatogram with retention times of 108, 110, and 114 min (Figure 2B), which were collected and identified using ESI-MS. The third fraction (i.e., P3) has a retention time identical to that of authentic PMal and contained no chemically modified peptides. The monoisotopic masses of the major peptides in peaks P1 and P2 were 921.3 ± 0.3 and 660.5 ± 0.3 Da, respectively, corresponding to the PMal-labeled peptides $L^{417}GMSCD^{422}$ and $C^{113}IE^{115}$ (Table 1). There is no ambiguity in this assignment, as there were no other peptides for which the theoretical masses were consistent with the measured masses. It is, therefore, apparent that PMal covalently modifies both Cys^{113} and Cys^{421}.

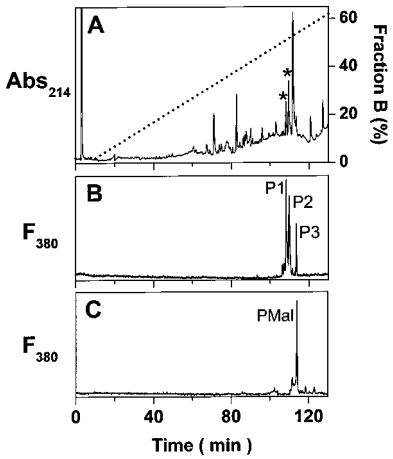

FIGURE 2: Reversed-phase HPLC separation of proteolytic fragments derived from PMal-AdoHcy hydrolase. PMal-labeled peptides initially isolated following chymotryptic digestion of AdoHcy hydrolase were pooled and subjected to a secondary digestion with endoproteinase Glu-C. Chromatogram representing the separation of PMal-labeled peptides generated from the secondary digestion (A, B) or using an authentic PMal standard (C), detected as the absorbance at 214 nm (A) or using a fluorescence detector (B, C), where $\lambda_{ex} = 340$ nm; $\lambda_{em} = 380$ nm. For details, see the text.

Table 1: Identification of PMal-Modified AdoHcy Hydrolase Peptides by ESI-MS[a]

retent time (min)	monoisotopic mass (Da)		peptide sequence[b]
	experimental	theoretical	
108	921.3	921.5	$L^{417}GMS\underline{\mathbf{C}}^{\mathbf{421}}D^{422}$
110	660.5	660.4	$\underline{\mathbf{C}}^{\mathbf{113}}IE^{115}$

[a] Theoretical monoisotopic masses corresponding to the expected proteolytic fragments of AdoHcy hydrolase were calculated from the cDNA-derived amino acid sequence (*16*). [b] Contains PMal, which has a monoisotopic mass of 297.3 Da.

Fluorescence Lifetimes and Rotational Dynamics of PMal Covalently Bound to AdoHcy Hydrolase. Frequency-domain measurements of the rotational dynamics of PMal-AdoHcy hydrolase require the measurement of the fluorescence lifetime. Therefore, the frequency-response of the phase delay and modulation of PMal bound to AdoHcy hydrolase were measured at 20 frequencies between 0.2 and 100 MHz (Figure 3). The intensity decay of PMal bound to AdoHcy hydrolase represents the weighted average of PMal bound to Cys^{113} and Cys^{421} and can be adequately described as a sum of four exponentials, as shown by the random distribution of the weighted residuals. The average fluorescence lifetime of PMal bound to AdoHcy hydrolase is approximately 50 ns at 25 °C (Table 2), which is sufficiently long for the measurement of both internal domain motions

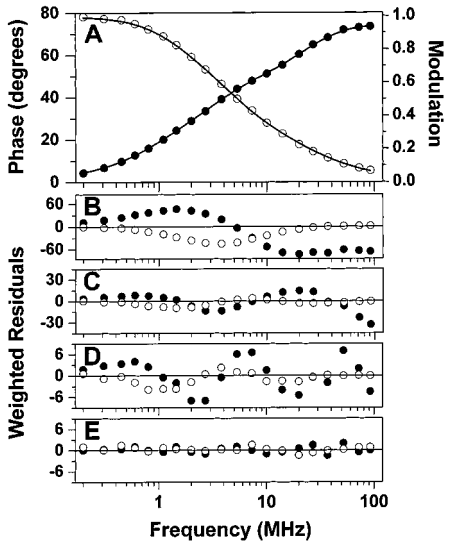

FIGURE 3: Lifetime data for PMal covalently bound to AdoHcy hydrolase. Frequency-response and four-exponential fit (solid lines) corresponding to the phase shift (●) and modulation (○) for PMal-AdoHcy hydrolase (0.05 mg mL^{-1}) in buffer A at 25 °C (A). Data were fit to a sum of exponentials, where $I(t) = \sum_i \alpha_i \tau_i$ The weighted residuals (i.e., the difference between the experimental data and the calculated fit divided by the experimental uncertainty) are shown for a one-exponential (B), two-exponential (C), three-exponential (D), and four-exponential (E) fit to the data. The respective χ_R^2 are 1444, 90, 12, and 1.4.

and the overall rotational motion of the AdoHcy hydrolase tetramer. It should be noted that in previous examples the fluorescence intensity decay of PMal bound to a single site on a protein or oligonucleotide have been adequately described by a three exponential decay (*22*−*25*). PMal is known to be highly sensitive to its local environment and would be expected to have different lifetime intensity decays depending on whether the chromophore was bound to a site near the protein surface or within an interior site (*26*, *27*). Therefore, the added complexity of the intensity decay of PMal bound to AdoHcy hydrolase is probably a reflection of increased structural heterogeneity resulting from differences in the environments of PMal bound to Cys^{113} and Cys^{421} (*28*).

Resolution of the rotational dynamics of PMal bound to AdoHcy hydrolase involved the measurement of the differential phase and modulated anisotropy between 0.2 and 100 MHz (Figure 4). In fitting the fluorescence anisotropy decay, we have assumed that the fluorescence intensity decay is representative of the PMal chromophores bound at both Cys^{113} and Cys^{421}. However, it should be emphasized that differences in the fluorescence intensity decays associated with PMal bound to each of these sites have the potential to result in systematic errors with respect to the determination of the rotational correlation times associated with AdoHcy hydrolase. Therefore, the fitting parameters determined from the fluorescence anisotropy decay represent a weighted average of PMal bound to multiple labeling sites. Nevertheless, qualitative differences in the fluorescence anisotropy decays resulting from ligand binding and oxidation provide reliable measurements of changes in the hydrodynamic properties of AdoHcy hydrolase, as indicated by the good agreement between the measured and calculated rotational correlation times associated with the overall rotational dynamics of AdoHcy hydrolase (see below).

The frequency-domain anisotropy decay of the substrate-free form of AdoHcy hydrolase can be adequately described as a sum of three exponentials, as shown by the randomly weighted residuals (Figure 4A). Therefore, prior to substrate binding, three rotational correlation times are observed centered at 1.3, 25, and 131 ns (Table 3). The longest rotational correlation time is consistent with the overall rotational motion of the tetrameric complex of AdoHcy hydrolase based on the theoretical rotational correlation times determined from the crystal structure using the program HYDROPRO (*8*, *29*). These calculations indicate that the expected rotational correlation times associated with different principal axes of the tetrameric complex are between 122 and 134 ns. On the other hand, the shorter rotational correlation times probably represent the segmental rotational dynamics of the pyrene chromophore and an independent domain motion within individual subunits in the complex. Since the overall rotational motion of a protein is sensitive to changes in size and shape (*30*), these fluorescence anisotropy measurements can be used to assess possible global conformational changes in the structure of the tetrameric complex of AdoHcy hydrolase induced by ligand binding and substrate oxidation.

The frequency-response of the differential phase and modulated anisotropy was therefore measured for AdoHcy hydrolase in the presence of saturating concentrations of the Ado analogue NepA (Figure 4D). NepA is irreversibly oxidized at the 3′-position of the cyclopentenyl ring to form the 3′-keto derivative with concomitant conversion of the enzyme from the NAD^+ to NADH form. Like DHCeA, the substrate used by Howell and coworkers to determine the crystal structure of AdoHcy hydrolase, the 3′-keto derivative of NepA is tightly bound to the NADH form of the enzyme (*7*, *31*, *32*). In the presence or absence of NepA, there is essentially no change in the excited-state lifetime of PMal (Table 2), indicating that the structure around Cys^{113} and Cys^{421} is not substantially perturbed following binding and oxidation of this substrate. The anisotropy decay is adequately described by two rotational correlation times centered at 2 and 101 ns (Table 3). This result is in contrast to the result obtained for the substrate-free form of AdoHcy hydrolase, where three rotational correlation times are necessary to describe the anisotropy decay (see above). The absence of a significant contribution to an intermediate rotational correlation time (i.e., $\phi_2 \approx 25$ ns) suggests that individual domain motions within AdoHcy hydrolase are substantially reduced following substrate binding and oxidation. The short rotational correlation time, corresponding to the segmental motion of the pyrene chromophore, is analogous to that observed for the substrate-free form of the enzyme and suggests that the conformations around Cys^{113} and Cys^{421} are unaffected. However, there is a substantial decrease in the rotational correlation time associated with the overall rotational dynamics of the tetrameric complex (i.e., from $\phi_3 = 131$ ns for the substrate-free enzyme to 101 ns following NepA binding and oxidation; Table 3). This rotational correlation time is consistent with the more compact (closed) structure observed in the crystal structure following substrate binding and oxidation, whose expected rotational correlation times for the different principal axes of rotation vary between 95 and 111 ns when calculated using the program HYDROPRO (*7*, *29*).

Table 2: Lifetime Data for PMal Covalently Bound on AdoHcy Hydrolase[a]

sample	α_1	τ_1 (ns)	α_2	τ_2 (ns)	α_3	τ_3 (ns)	α_4	τ_4 (ns)	$<\tau>$ (ns)	χ_R^2
E_{NAD+}	0.27	1.4	0.42	9	0.23	37	0.08	106	59	6.5
	(0.23−0.31)[b]	(0.4−2.1)	(0.37−0.45)	(7−11)	(0.19−0.27)	(26−47)		(94−129)		
E_{NAD+}	0.28	2.1	0.36	10	0.28	36	0.08	97	52	4.5
+ 3′-deoxyAdo	(0.20−0.36)	(1.2−2.8)	(0.28−0.41)	(6−13)	(0.22−0.33)	(26−50)		(80−142)		
E_{NAD+}/E_{NADH}	0.26	1.8	0.40	9	0.27	35	0.07	97	51	3.7
+ Ado/3′-ketoAdo	(0.21−0.33)	(1.0−2.5)	(0.34−0.44)	(6−11)	(0.23−0.31)	(27−45)		(81−129)		
E_{NADH}	0.29	1.8	0.40	9	0.25	33	0.06	103	50	3.3
+ 3′-ketoNepA	(0.23−0.34)	(1.2−2.4)	(0.35−0.44)	(7−11)	(0.21−0.29)	(26−42)		(89−126)		

[a] Parameters are derived from simultaneously fitting 3−4 data sets for PMal-AdoHcy hydrolase (0.05 mg mL^{-1}) in buffer A and 1.0 mM of 3′-deoxyAdo, Ado, or NepA, where $I(t) = \sum_i \alpha_i \tau_i$ and the average lifetime $<\tau>$ equals: $<\tau> = \sum_i \alpha_i \tau_i^2 / \sum_i \alpha_i \tau_i$. [b] Numbers in parentheses represent the variance associated with a rigorous analysis of the correlated errors between the seven fitting parameters relative to the parameter of interest, as previously described (*42*).

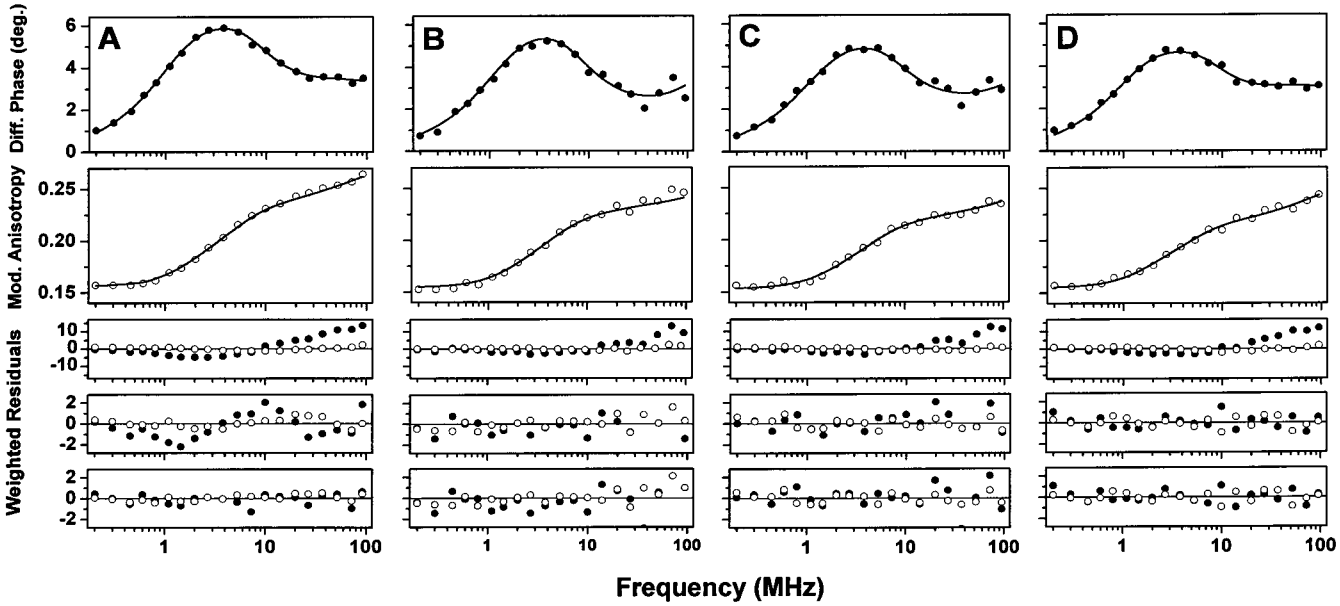

FIGURE 4: Fluorescence anisotropy decay for PMal-AdoHcy hydrolase. Differential phase angle (●) and modulated anisotropy (○) data and nonlinear least-squares fits (solid lines) prior to substrate binding (A) or following the addition of 1.0 mM 3′-deoxyAdo (B), Ado (C), or NepA (D). Weighted residuals are shown below the respective data sets and correspond to a one-exponential (top), two-exponential (middle), and three-exponential (bottom) fit to the data. The respective χ_R^2 are 24, 1.0, and 0.2 (A); 12, 1.0, and 1.0 (B); 11, 1.4, and 1.5 (C); and 14, 0.4, and 0.4 (D). Experimental conditions are as described in the legend to Figure 3.

Table 3: Rotational Dynamics of PMal Labeled on AdoHcy Hydrolase[a]

sample	r_0[b]	g_1	ϕ_1 (ns)	g_2	ϕ_2 (ns)	g_3	ϕ_3 (ns)	χ_R^2
E_{NAD+}	0.29	0.15	1.3	0.21	25	0.64	131	0.3
	(0.28−0.30)	(0.14−0.17)	(0.8−1.7)	(0.14−0.38)	(15−42)		(113−182)	
E_{NAD+}	0.29	0.16	1.0			0.84	99	2.0
+ 3′-deoxyAdo	(0.27−0.31)	(0.15−0.17)	(0.8−1.1)				(93−104)	
E_{NAD+}/E_{NADH}	0.26	0.15	1.2			0.85	91	0.9
+ Ado/3′-ketoAdo	(0.25−0.28)	(0.13−0.19)	(0.7−1.8)				(86−95)	
E_{NADH}	0.26	0.17	2.1			0.83	101	0.9
+ 3′-ketoNepA	(0.25−0.27)	(0.16−0.18)	(1.6−2.5)				(96−106)	

[a] Parameters are derived from simultaneously fitting 3−4 data sets for PMal-AdoHcy hydrolase (0.05 mg mL^{-1}) in buffer A and 1.0 mM of 3′-deoxyAdo, Ado, or NepA, where $A(t) = r_0 \sum_i g_i \exp(-t/\phi_i)$. [b] r_0 is the initial anisotropy at time zero. Numbers in parentheses represent the variance associated with a rigorous analysis of the correlated errors between the seven fitting parameters relative to the parameter of interest, as previously described (*42*).

To address whether ligand binding or oxidation is responsible for the global structural rearrangement within AdoHcy hydrolase, we have measured the rotational dynamics following binding of the natural substrate Ado and the nonoxidizable analogue 3′-deoxyAdo. In both cases, the fluorescence anisotropy decay following ligand binding is analogous to that observed following incubation with NepA and is adequately described by two rotational correlation times (Figure 4, panels B and C; Table 3). These results indicate that ligand binding results in global structural changes within the AdoHcy hydrolase tetramer and that oxidation of the substrate and the resultant formation of NADH do not significantly alter the overall hydrodynamic properties of the enzyme complex.

Dynamic Structure of the Carboxyl-Terminal Domain of AdoHcy Hydrolase. While the long excited-state lifetime of PMal is ideal for the detection of the overall rotational dynamics of AdoHcy hydrolase, the chemical modification

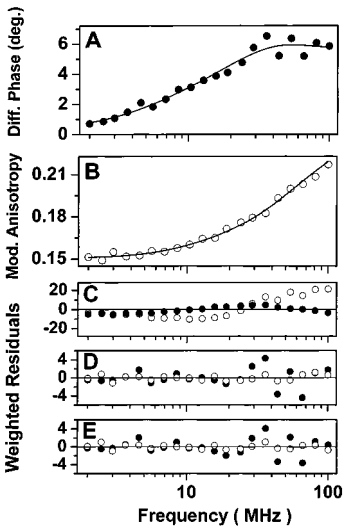

FIGURE 5: Fluorescence anisotropy decay of AEDANS-AdoHcy hydrolase. Top panels illustrate the frequency-dependent differential phase angle (A; ●) and modulated anisotropy (B; ○) for AEDANS-AdoHcy hydrolase. Lines represent the nonlinear least-squares fit to the data. Bottom panels show the weighted residuals for a one-exponential (C), two-exponential (D), and three-exponential (E) nonlinear least-squares fit to the data. The respective χ_R^2 are 68 (C), 2.2 (D), and 2.0 (E). Experimental conditions are as described in the legend to Figure 3.

of Cys^{113} within the catalytic domain and Cys^{421} in the carboxyl-terminal domain prevents an unambiguous interpretation of the origin of the intermediate rotational correlation time observed for the substrate-free form of AdoHcy hydrolase (Table 3). We have, therefore, covalently modified AdoHcy hydrolase using IAEDANS in the presence of Ado, resulting in the modification of a single site on the enzyme. This latter observation is in agreement with earlier data using DTNB and iodoacetamide, which selectively modify the surface exposed Cys^{421} within the carboxyl-terminal domain (*11*). It is apparent that IAEDANS preferentially modifies Cys^{421} within the carboxyl-terminal domain, where the polarity of IAEDANS prevents this chromophore from partitioning into the more hydrophobic site in the vicinity of Cys^{113} in the presence of Ado. It should be noted that AEDANS is only suitable for measurements prior to substrate oxidation, as the fluorescence emission of NADH following substrate oxidation overlaps that of AEDANS.

The excited state lifetime and anisotropy decay of AEDANS bound to AdoHcy hydrolase was measured prior to substrate binding. The fluorescence intensity decay is adequately described as a sum of two exponentials (i.e., $\alpha_1 = 0.27 \pm 0.01$; $\tau_1 = 2.1 \pm 0.3$ ns; and $\tau_2 = 15.2 \pm 0.02$ ns). Therefore, the excited state lifetime is apparently appropriate for the accurate detection of domain motions associated with the carboxyl-terminal domain. The differential phase and modulated anisotropy of AEDANS-AdoHcy hydrolase were measured over 20 frequencies between 2 and 100 MHz to assess the rotational dynamics of the carboxyl-terminal domain (Figure 5). The data require two exponentials to be adequately fit, as is evidenced by the evenly distributed weighted residuals and a 30-fold reduction of χ_R^2 relative to the one-exponential model. There is no improvement in the calculated fit to the data with additional fitting parameters. The two rotational correlation times (i.e., $\phi_1 = 2.4 \pm 0.3$ ns and $\phi_2 = 114 \pm 24$ ns) correspond to the segmental motion of the AEDANS chromophore and the overall rotational motion of the tetrameric AdoHcy hydrolase. We emphasize that the longer rotational correlation time, corresponding to the overall rotational dynamics of the tetramer, is within the experimental error of the measurement obtained using PMal to label AdoHcy hydrolase (Table 3). Thus, using two different chromophores similar results are obtained. These results indicate that the carboxyl-terminal domain undergoes no significant independent motion and is tightly associated with the tetrameric complex. It should be noted that these results are consistent with the extensive hydrogen bonding between side chains near the carboxyl-terminus and residues within the NAD^+ binding domain and the role of the carboxyl-terminal domain in forming a binding pocket for NAD^+ (*7*, *8*). Furthermore, these results strongly suggest that the intermediate rotational correlation time associated with domain motions within AdoHcy hydrolase following PMal modification is associated with the catalytic domain. Therefore, prior to substrate binding the catalytic domain undergoes large amplitude domain motions around a hinge element in the structure, which are dramatically reduced following ligand binding.

DISCUSSION

Summary of Results. The oxidative and hydrolytic activities of AdoHcy hydrolase are retained following covalent modification of selected cysteines with either PMal or IAEDANS, permitting the measurement of catalytically important global conformational changes associated with substrate binding and oxidation. There is a significant decrease in the overall rotational correlation time of AdoHcy hydrolase following the binding and oxidation of the Ado analogue NepA, indicating that the hydrodynamic radius of the tetramer becomes smaller (*30*). This result is consistent with observed differences between the available structures of AdoHcy hydrolase crystalized in both a substrate-free, NAD^+ form (*8*), and a substrate-bound (3′-ketoDHCeA), NADH form (*7*) (Figure 1). Significantly, our results demonstrate that ligand binding results in a large conformational reorientation within the tetramer, while substrate oxidation and the resultant formation of NADH have no measurable effect on the hydrodynamic properties of the enzyme (Table 3). Furthermore, prior to ligand binding the catalytic domain undergoes large amplitude motions. These latter results indicate the presence of a flexible hinge element between the catalytic and the NAD^+ binding domains (*33*−*35*). Following ligand binding, the independent rotational motion of the catalytic domain is essentially abolished, suggesting that ligand binding results in closure of the active site, which brings the catalytic and the NAD^+ binding domains into contact with one another. In contrast, the small carboxyl-terminal domain undergoes essentially no independent rotational motion relative to the tetrameric complex, consistent with the structural role of the carboxyl-terminus in defining part of the binding pocket for NAD^+ (*7*, *8*). Because the NAD^+ cofactor and substrate binding sites are found within the crevice between the catalytic and the NAD^+ domains, these results suggest that substrate binding stabilizes a closed conformation, which positions catalytic groups around the substrate.

Relationship to Other Work. The tertiary structure of the catalytic domain of AdoHcy hydrolase contains a well-

defined binding site for AdoHcy (*7*, *8*). On the basis of molecular modeling arguments, Takusagawa and coworkers suggested that AdoHcy binding should require no major conformational changes in the "open" structure of AdoHcy hydrolase and that small changes in the conformation of the carboxyl-terminal domain following substrate binding may trigger domain closure (*8*). In contrast, large amplitude motions associated with the catalytic domain determined in solution prior to substrate binding would allow such inter-domain contact (see Table 3). A more detailed analysis of the structure of the NADH form of AdoHcy hydrolase bound to 3′-ketoDHCeA reveals that amino acid side chains located in both the catalytic and NAD^+ binding domains contribute to the substrate binding site (*5*, *7*). This structural observation is consistent with the present study and suggests that the catalytic and the NAD^+ binding domains are stabilized to form a closed active site through the interactions with the substrate prior to substrate oxidation. Furthermore, since closure of the active site appears to involve a rigid body motion of the catalytic and NAD^+ binding domains to poise the geometry of Ado and NAD^+ for catalysis, it is likely that the high-resolution structure of the NADH form of AdoHcy hydrolase bound to 3′-ketoDHCeA can be used in the design of effective enzyme inhibitors.

A similar reduction in large-amplitude hinge bending motions upon substrate binding has been reported in other proteins, which also contain substrate binding elements within two large domains, including calmodulin, galactose-glucose binding protein, and maltose-binding protein (*23*, *24*, *33*−*40*). As is the case for AdoHcy hydrolase, substrate binding functions to directly restrict the rotational dynamics of domain elements so as to define the active protein conformation. This mechanism, involving a rigid domain motion to form the substrate binding site, is consistent with earlier suggestions that ligand binding can function to modify a dynamic equilibrium between different protein states in which a fraction of the binding energy is used to stabilize the protein into a compact state, thereby preventing release of the ligand during catalysis (*40*, *41*).

Conclusions and Future Directions. Large amplitude domain motions involving the catalytic domain of AdoHcy hydrolase are essentially eliminated upon ligand binding, resulting in closure of the active site to engulf the substrates during catalysis. Future experiments should focus on defining the hinge element associated with the independent rotational dynamics of the catalytic domain, which will permit an assessment of the role of domain mobility in the catalytic mechanism of AdoHcy hydrolase. Other open questions that remain for future study are to define (i) whether substrate may initially interact with a specific domain prior to high affinity binding and (ii) the extent of the structural changes that occur upon oxidation of ligands such as Ado and NepA, which might serve to isolate reactive intermediates within the active site to prevent abortive side reactions.

ACKNOWLEDGMENT

We thank P. Lynne Howell and Diana J. Bigelow for insightful discussions, Michael S. Hershfield for providing a clone overexpressing human placental AdoHcy hydrolase, and José Carcía de La Torre for assisting us calculating the hydrodynamic properties of AdoHcy hydrolase. We thank Todd D. Williams and Homigol Biesiada of the KU Mass Spectrometry Laboratory for their efforts in acquiring the ESI-MS spectrum.

REFERENCES

1. Chiang, P. K., Gordon, R. K., Tal, J., Zeng, G. C., Doctor, B. P., Pardhasaradhi, K., and McCann, P. P. (1996) *FASEB J. 10*, 471−480.
2. Smolin, L. A., and Benevenga, N. J. (1989) in *Absorption and Utilization of Amino Acids* (Friedman, M., Ed.) pp 157−187, CRC Press, Inc., Boca Raton, FL.
3. Dimmock, N. J., and Primrose, S. B. (1994) *Introduction of Modern Virology*, Blackwell Sciences, London.
4. Narayan, P., and Rottman, F. M. (1992) in *Advances in Enzymology* (Meister, A., Ed.) pp 255−285, John Wiley & Sons Inc., New York.
5. Yin, D., Yang, X., Borchardt, R. T., and Yuan, C.-S. (2000) in *Biomedical Chemistry: Applying Chemical Principles to the Understanding and Treatment of Disease* (Torrence, P. F., Ed.) pp 41−71, John Wiley & Sons, Inc., New York.
6. Nygard, O., Vollset, S. E., Refsum, H., Brattstrom, L., and Ueland, P. M. (1999) *J. Intern. Med. 246*, 425−454.
7. Turner, M. A., Yuan, C.-S., Borchardt, R. T., Hershfield, M. S., Smith, G. D., and Howell, P. L. (1998) *Nat. Struct. Biol. 5*, 369−376.
8. Hu, Y., Komoto, J., Huang, Y., Gomi, T., Ogawa, H., Takata, Y., Fujioka, M., and Takusagawa, F. (1999) *Biochemistry 38*, 8323−8333.
9. Ault-Riché, D. B., Yuan, C.-S., and Borchardt, R. T. (1994) *J. Biol. Chem. 269*, 31472−31478.
10. Yuan, C.-S., Wnuk, S. F., Liu, S., Robins, M. J., and Borchardt, R. T. (1994) *Biochemistry 33*, 12305−12311.
11. Yuan, C.-S., Ault-Riché, D. B., and Borchardt, R. T. (1996) *J. Biol. Chem. 271*, 28009−28016.
12. Bradford, M. M. (1976) *Anal. Biochem. 72*, 248−254.
13. Haugland, R. P. (1996) *Handbook of Fluorescent Probes and Research Chemicals*, 6th ed., Molecular Probes Inc., Eugene, OR.
14. Gao, J., Yin, D., Yao, Y., Williams, T. D., and Squier, T. C. (1998) *Biochemistry 37*, 9536−9548.
15. Gao, J., Yin, D. H., Yao, Y., Sun, H., Qin, Z., Schöneich, C., Williams, T. D., and Squier, T. C. (1998) *Biophys. J. 74*, 1115−1134.
16. Coulter-Karis, D. E., and Hershfield, M. S. (1989) *Ann. Hum. Genet. 53*, 169−175.
17. Bevington, P. R. (1969) *Data Reduction and Error Analysis for the Physical Sciences*, McGraw-Hill, New York.
18. Weber, G. (1981) *J. Phys. Chem. 85*, 949−953.
19. Lakowicz, J. R., Cherek, H., and Maliwal, B. P. (1985) *Biochemistry 24*, 376−383.
20. Johnson, M. L., and Faunt, L. M. (1992) *Methods Enzymol. 210*, 1−37.
21. Hunter, G. W., and Squier, T. C. (1998) *Biochim. Biophys. Acta 1415*, 63−76.
22. Yguerabide, J., Talavera, E., Alvarez, J. M., and Afkir, M. (1996) *Anal. Biochem. 241*, 238−247.
23. Yao, Y., Schoneich, C., and Squier, T. C. (1994) *Biochemistry 33*, 7797−7810.
24. Yao, Y., and Squier, T. C. (1996) *Biochemistry 35*, 6815−6827.
25. Benfenati, F., Neyroz, P., Bahler, M., Masotti, L., and Greengard, P. (1990) *J. Biol. Chem. 265*, 12584−12595.
26. Weltman, J. K., Szaro, R. P., Frackelton, A. R., Jr., Dowben, R. M., Bunting, J. R., and Cathou, B. E. (1973) *J. Biol. Chem. 248*, 3173−3177.
27. Vaughan, W. M., and Weber, G. (1970) *Biochemistry 9*, 464−473.
28. Royer, C. A. (1993) *Biophys. J. 65*, 9−10.
29. García de la Torre, J., Huertas, M. L., and Carrasco, B. (2000) *Biophys. J. 78*, 719−730.

30. Steiner, R. F. (1991) in *Topics in Fluorescence Spectroscopy* (Lakowicz, J. R., Ed.) pp 1−52, Plenum Press, New York.
31. Matuszewska, B., and Borchardt, R. T. (1987) *J. Biol. Chem. 262*, 265−268.
32. Paisley, S. D., Wolfe, M. S., and Borchardt, R. T. (1989) *J. Med. Chem. 32*, 1415−1418.
33. Gerstein, M., Lesk, A. M., and Chothia, C. (1994) *Biochemistry 33*, 6739−6749.
34. Gerstein, M., and Krebs, W. (1998) *Nucleic Acids Res. 26*, 4280−4290.
35. Subbiah, S. (1996) *Protein Motions* pp 41−71, R. G. Landes Co., Austin, TX.
36. Sharff, A. J., Rodseth, L. E., Spurlino, J. C., and Quiocho, F. A. (1992) *Biochemistry 31*, 10657−10663.
37. Barbato, G., Ikura, M., Kay, L. E., Pastor, R. W., and Bax, A. (1992) *Biochemistry 31*, 5269−5278.
38. Careaga, C. L., Sutherland, J., Sabeti, J., and Falke, J. J. (1995) *Biochemistry 34*, 3048−3055.
39. Sun, H., Yin, D., and Squier, T. C. (1999) *Biochemistry 38*, 12266−12279.
40. Döring, K., Surrey, T., Nollert, P., and Jähnig, F. (1999) *Eur. J. Biochem. 266*, 477−483.
41. Frauenfelder, H., Parak, F., and Young, R. D. (1988) *Annu. Rev. Biophys. Biophys. Chem. 17*, 451−479.
42. Beechem, J. M., Gratton, E., Ameloot, M., Knutson, J. R., and Brand, L. (1991) in *Topics in Fluorescence Spectroscopy* (Lakowicz, J. R., Ed.) pp 241−306, Plenum Press, New York.
43. Palmer, J. L., and Abeles, R. H. (1979) *J. Biol. Chem. 254*, 1217−1226.

BI000595A